SeDIF Conference

International Conference on
Seismic Design of Industrial Facilities
2013, RWTH Aachen University

The Scaled Boundary Finite Element Method for Transient Wave Propagation Problems

Carolin Birk[1], Denghong Chen[2], Chongmin Song[1] and Chengbin Du[3]

[1] School of Civil and Environmental Engineering, University of New South Wales, Sydney NSW 2052, Australia
c.birk@unsw.edu.au; c.song@unsw.edu.au

[2] College of Civil Engineering and Architecture, China Three Gorges University, Yichang 443002 China

[3] Department of Engineering Mechanics, Hohai University, Nanjing 210098 China

ABSTRACT:

A high-order time-domain approach for wave propagation in bounded and unbounded domains is developed based on the scaled boundary finite element method. The dynamic stiffness matrices of bounded and unbounded domains are expressed as continued-fraction expansions. The coefficient matrices of the expansions are determined recursively. This approach leads to accurate results with only about 3 terms per wavelength. A scheme for coupling the proposed high-order time-domain formulation for bounded domains with a high-order transmitting boundary suggested previously is also proposed. In the time-domain, the coupled model corresponds to equations of motion with symmetric, banded and frequency-independent coefficient matrices, which can be solved efficiently using standard time-integration schemes. A numerical example is presented.

Keywords: dynamic soil-structure interaction, wave propagation, scaled boundary finite element method, continued fractions

1 Introduction

The modelling of wave propagation is essential in a dynamic soil-structure interaction analysis. This is associated with two major challenges: the unbounded extent of the soil and fine mesh requirements for high-frequency components. Numerical methods for wave propagation in unbounded domains include absorbing boundaries [1, 2], the boundary element method [3, 4], infinite elements [5], the thin-layer method [6] and perfectly matched layers [7]. For extensive reviews of these methods the reader is referred to References [8, 9]. For wave propagation in bounded domains, spectral elements [10, 11] have been proven to be efficient.

S. Klinkel et al. (Eds.), *Seismic Design of Industrial Facilities*,
DOI 10.1007/978-3-658-02810-7_45, © Springer Fachmedien Wiesbaden 2014

A relatively recent method that combines the advantages of accurately modelling radiation damping and employing spectral element concepts is the scaled boundary finite element method [12]. This semi-analytical technique also excels in modelling singularities and can thus be used to model the propagation of seismic waves in the ground containing faults or discontinuities. The original solution procedure of the scaled boundary finite element method has been developed in the frequency domain [13]. Time-domain solutions have thus been obtained using inverse Fourier transformation and evaluating convolution integrals in early publications.

Recently, efficient direct time-domain formulations of the scaled boundary finite element method have been proposed in References [14, 15] for unbounded and bounded domains, respectively. These are based on continued-fraction solutions of the scaled boundary finite element equation in dynamic stiffness. Although these approaches are conceptually appealing, they have only been applied to problems with a small number of degrees of freedom in References [14, 15]. The extension to large scale problems is challenging, due to potential ill-conditioning of the original continued-fraction algorithms. In Reference [16] an improved, numerically more robust continued-fraction expansion technique has been proposed for unbounded domains by introducing an additional scaling. The improved continued-fraction solution is extended to wave propagation problems in bounded domains in this paper. The coupling of the resulting time-domain model for bounded domains with the transmitting boundary derived in Reference [16] is also addressed. Finally, a robust unified high-order time-domain formulation of the scaled boundary finite element method is established, that can be used for the direct time-domain analysis of complex coupled soil-structure systems containing singularities.

2 Concept of the scaled boundary finite element method

In the scaled boundary finite element method, a so-called scaling centre O is chosen in a zone from which the total boundary, other than the straight surfaces passing through the scaling centre, must be visible (Figures 1(a) and 1(b)). Only the boundary S is discretized. A typical line element to be used in a two-dimensional analysis is shown in Figure 1(c). The scaled boundary transformation (Eq. (1)) relating the Cartesian coordinates $\hat{x}$, $\hat{y}$, $\hat{z}$ to the scaled boundary coordinates ξ, η, ζ is introduced. Here, the symbols $\{x\}$, $\{y\}$, $\{z\}$ and $[N(\eta,\zeta)]$ denote nodal coordinates and shape functions of isoparametric elements, respectively.

$$\begin{aligned} \{\hat{x}(\xi,\eta,\zeta)\} &= \xi[N(\eta,\zeta)]\{x\} \\ \{\hat{y}(\xi,\eta,\zeta)\} &= \xi[N(\eta,\zeta)]\{y\} \\ \{\hat{z}(\xi,\eta,\zeta)\} &= \xi[N(\eta,\zeta)]\{z\} \end{aligned} \tag{1}$$

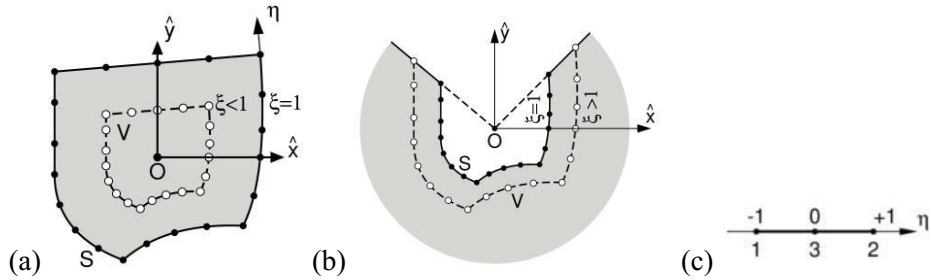

Figure 1: Concept of scaled boundary finite element method: (a) bounded domain, (b) unbounded domain, (c) 3-node line element on boundary

The displacements at a point (ξ, η, ζ) are obtained interpolating nodal displacements $\{u(\xi)\}$ using the same shape functions as for the geometry.

$$\{u(\xi,\eta,\zeta)\} = [N(\eta,\zeta)]\{u(\xi)\} \tag{2}$$

Applying the method of weighted residuals to the governing equations formulated in terms of the scaled boundary coordinates, the scaled boundary finite element equation in displacements $\{u(\xi)\}$ is obtained.

$$[E^0]\xi^2\{u(\xi)\}_{,\xi\xi} + \big((s-1)[E^0] - [E^1] + [E^1]^T\big)\xi\{u(\xi)\}_{,\xi} + \big((s-2)[E^1]^T - [E^2]\big)\{u(\xi)\} + \omega^2[M^0]\xi^2\{u(\xi)\} = 0 \tag{3}$$

The coefficient matrices $[E^0]$, $[E^1]$, $[E^2]$ and $[M^0]$ are evaluated using standard finite element technologies [13]. The dynamic stiffness $[S(\omega)]$ relates the amplitudes of the nodal forces $\{R(\omega)\}$ to the amplitudes of the nodal displacements $\{u(\omega)\}$ at the boundary.

$$\{R(\omega)\} = [S(\omega)]\{u(\omega)\} \tag{4}$$

Using the relationship between internal nodal forces and nodal displacements, Equation (3) can be transformed into an equivalent differential equation in $[S(\omega)]$, the so-called scaled boundary finite element equation in dynamic stiffness.

$$(\pm[S(\omega)] - [E^1])[E^0]^{-1}(\pm[S(\omega)] - [E^1]^T) \pm (s-2)[S(\omega)] \pm \omega[S(\omega)]_{,\omega} - \big[E^{\{2\}}\big] + \omega^2[M^0] = 0 \tag{5}$$

Equation (5) is valid for both bounded and unbounded domains, where the upper and lower signs apply in the bounded and unbounded case, respectively.

3 Bounded domains

A high-order time domain formulation for bounded domains can be constructed by expanding the dynamic stiffness $[S^b(\omega)]$ into a series of continued fractions.

3.1 Continued-fraction expansion of dynamic stiffness matrix

The dynamic stiffness at the boundary is expressed as

$$[S^b(\omega)] = [K] - \omega^2[M] - \omega^4\left[X^{(1)}\right]\left[S^{(1)}(\omega)\right]^{-1}\left[X^{(1)}\right]^T, \tag{6}$$

where a scaling factor $\left[X^{(1)}\right]$ is introduced to improve the numerical condition of the solution. Equations for the coefficient matrices in Equation (6) are obtained by substituting it in Equation (5) and setting individual terms corresponding to powers of ω^2 to zero in ascending order. The constant term yields an equation for the static stiffness matrix $[K]$,

$$([K] - [E^1])[E^0]^{-1}([K] - [E^1]^T) - [E^2] + (s-2)[K] = 0. \tag{7}$$

An equation for the mass matrix $[M]$ is obtained by setting the terms in ω^2 equal to zero.

$$([K] - [E^1])[E^0]^{-1}[M] + [M][E^0]^{-1}([K] - [E^1]^T) + s[M] - [M^0] = 0 \tag{8}$$

The remaining terms yield an equation for the residual $\left[S^{(i)}(\omega)\right]$ (with $i = 1$),

$$\begin{aligned}&\left[S^{(i)}(\omega)\right]\left[c^{(i)}\right]\left[S^{(i)}(\omega)\right] - \left[S^{(i)}(\omega)\right]\left[b_0^{(i)}\right]^T - \left[b_0^{(i)}\right]\left[S^{(i)}(\omega)\right] + \\ &\omega^2\left(\left[S^{(i)}(\omega)\right]\left[b_1^{(i)}\right]^T + \left[b_1^{(i)}\right]\left[S^{(i)}(\omega)\right]\right) + \omega\left[S^{(i)}(\omega)\right]_{,\omega} + \omega^4\left[a^{(i)}\right] = 0,\end{aligned} \tag{9}$$

with the constants

$$\begin{aligned}\left[a^{(1)}\right] &= \left[X^{(1)}\right]^T[E^0]^{-1}\left[X^{(1)}\right],\\ \left[b_0^{(1)}\right] &= \left[X^{(1)}\right]^T[E^0]^{-1}([K] - [E^1]^T)\left[X^{(1)}\right]^{-T} - (s+2)/2[I],\\ \left[b_1^{(1)}\right] &= \left[X^{(1)}\right]^T[E^0]^{-1}[M]\left[X^{(1)}\right]^{-T},\\ \left[c^{(1)}\right] &= \left[X^{(1)}\right]^{-1}[M][E^0]^{-1}[M]\left[X^{(1)}\right]^{-T}.\end{aligned} \tag{10}$$

The parameter $\left[X^{(1)}\right]$ is selected in such a way that $\left[c^{(1)}\right]$ is a diagonal matrix with entries +1 or -1.

Similarly, Eq. (9) is solved by postulating

$$\left[S^{(i)}(\omega)\right] = \left[S_0^{(i)}\right] - \omega^2\left[S_1^{(i)}\right] - \omega^4\left[X^{(i+1)}\right]\left[S^{(i+1)}(\omega)\right]^{-1}\left[X^{(i+1)}\right]^T \tag{11}$$

The solution for $\left[S_0^{(i)}\right]$ is obtained from

$$\left[S_0^{(i)}\right]^{-1}\left[b_0^{(i)}\right] + \left[b_0^{(i)}\right]^T\left[S_0^{(i)}\right]^{-1} = \left[c^{(i)}\right]. \tag{12}$$

The solution for $\left[S_0^{(i)}\right]$ follows from

$$\left(-\left[b_0^{(i)}\right]+\left[S_0^{(i)}\right]\left[c^{(i)}\right]\right)\left[S_1^{(i)}\right]+\left[S_1^{(i)}\right]\left(-\left[b_0^{(i)}\right]^T+\left[c^{(i)}\right]\left[S_0^{(i)}\right]\right)+$$
$$2\left[S_1^{(i)}\right]=\left[b_1^{(i)}\right]\left[S_0^{(i)}\right]+\left[S_0^{(i)}\right]\left[b_1^{(i)}\right]^T. \tag{13}$$

The equation for $\left[S^{(i+1)}(\omega)\right]$ is the same as Eq. (9) with i replacing $i+1$ and the corresponding coefficient matrices

$$\begin{aligned}
\left[a^{(i+1)}\right]&=\left[X^{(i+1)}\right]^T\left[c^{(i)}\right]\left[X^{(i+1)}\right]\\
\left[b_0^{(i+1)}\right]&=\left[X^{(i+1)}\right]^T\left(2[I]-\left[b_0^{(i)}\right]^T+\left[c^{(i)}\right]\left[S_0^{(i)}\right]\right)\left[X^{(i+1)}\right]^{-T}\\
\left[b_1^{(i+1)}\right]&=\left[X^{(i+1)}\right]^T\left(-\left[b_1^{(i)}\right]^T+\left[c^{(i)}\right]\left[S_1^{(i)}\right]\right)\left[X^{(i+1)}\right]^{-T}\\
\left[c^{(i+1)}\right]&=\left[X^{(i+1)}\right]^{-1}\left(\left[a^{(i)}\right]-\left[b_1^{(i)}\right]\left[S_1^{(i)}\right]-\left[S_1^{(i)}\right]\left[b_1^{(i)}\right]^T\right.\\
&\quad\left.+\left[S_1^{(i)}\right]\left[c^{(i)}\right]\left[S_1^{(i)}\right]\right)\left[X^{(i+1)}\right]^{-T}
\end{aligned} \tag{14}$$

Therefore, Equation (9) can be solved recursively for high-order terms with the coefficient matrices updated by Equation (14). The LDL^T decomposition [17] of the coefficient $\left[c^{(i)}\right]$ is used to determine the scaling factor $\left[X^{(i)}\right]$. It is chosen as the lower diagonal matrix $\left[L^{(i)}\right]$, which can be normalized such that the diagonal entries of $\left[D^{(i)}\right]=\pm 1$.

$$\left[c^{(i)}\right]=\left[X^{(i)}\right]^{-1}\left[\tilde{c}^{(i)}\right]\left[X^{(i)}\right]^{-T},\quad \left[\tilde{c}^{(i)}\right]=\left[L^{(i)}\right]\left[D^{(i)}\right]\left[L^{(i)}\right]^T \tag{15}$$

3.2 High-order time-domain formulation

Starting from the continued-fraction solutions of the dynamic stiffness matrix, high-order time-domain formulations can be constructed as equations of motion describing bounded domains. Substituting Eq. (6) into Eq. (4), the force-displacement relationship is expressed as

$$\{R(\omega)\}=([K]-\omega^2[M])\{u(\omega)\}+\omega^2\left[X^{(1)}\right]\left\{u^{(1)}(\omega)\right\} \tag{16}$$

where the auxiliary variable $\left\{u^{(1)}(\omega)\right\}$ is defined as the case $i=1$ of

$$-\omega^2\left[X^{(i)}\right]^T\left\{u^{(i-1)}(\omega)\right\}=\left[S^{(i)}(\omega)\right]\left\{u^{(i)}(\omega)\right\} \tag{17}$$

with $\{u(\omega)\}=\left\{u^{(0)}(\omega)\right\}$. Substituting Eq. (11) into Eq. (17) leads to

$$\omega^2\left[X^{(i)}\right]^T\{u^{(i-1)}(\omega)\} + \left(\left[S_0^{(i)}\right] - \omega^2\left[S_1^{(i)}\right]\right)\{u^{(i)}(\omega)\} + \omega^2\left[X^{(i+1)}\right]\{u^{(i+1)}(\omega)\} = 0 \tag{18}$$

Equations (16) and (18) are easily written in the time domain as

$$\begin{aligned}\{R(t)\} &= [K]\{u(t)\} + [M]\{\ddot{u}(t)\} - \left[X^{(1)}\right]\{\ddot{u}^{(1)}(t)\} \\ 0 &= -\left[X^{(i)}\right]^T\{\ddot{u}^{(i-1)}(t)\} + \left[S_0^{(i)}\right]\{u^{(i)}(t)\} + \left[S_1^{(i)}\right]\{\ddot{u}^{(i)}(t)\} \\ &\quad - \left[X^{(i+1)}\right]\{\ddot{u}^{(i+1)}(t)\}\end{aligned} \tag{19}$$

An order M_b continued fraction expansion is terminated with the assumption $\{u^{(M_b+1)}(t)\} = 0$.

4 Unbounded domains

A detailed derivation for the improved continued fraction solution of the dynamic stiffness of an unbounded domain is presented in Reference [16]. It is obtained in the same way as for the bounded domain but at the high frequency limit. The continued fraction solution is postulated as

$$\begin{aligned}[S^{\infty}(\omega)] &= i\omega[C_{\infty}] + [K_{\infty}] - \left[X_u^{(1)}\right]\left[Y^{(1)}(\omega)\right]^{-1}\left[X_u^{(1)}\right]^T \\ \left[Y^{(i)}(\omega)\right] &= i\omega\left[Y_1^{(i)}\right] + \left[Y_0^{(i)}\right] - \left[X_u^{(i+1)}\right]\left[Y^{(i+1)}(\omega)\right]^{-1}\left[X_u^{(i+1)}\right]^T\end{aligned} \tag{20}$$

Substituting into Eq. (4), the force-displacement relationship is expressed in the time domain as

$$\begin{aligned}\{R(t)\} &= [C_{\infty}]\{\dot{u}(t)\} + [K_{\infty}]\{u(t)\} - \left[X_u^{(1)}\right]\{v^{(1)}(t)\} \\ 0 &= -\left[X_u^{(i)}\right]^T\{\dot{v}^{(i-1)}(t)\} + \left[Y_1^{(i)}\right]\{\dot{v}^{(i)}(t)\} + \left[Y_0^{(i)}\right]\{v^{(i)}(t)\} \\ &\quad - \left[X_u^{(i+1)}\right]\{v^{(i+1)}(t)\}\end{aligned} \tag{21}$$

where $\{v^{(i)}(t)\}$ are auxiliary variables. An order M_u continued fraction expansion is terminated with the assumption $\{u^{(M_u+1)}(t)\} = 0$.

5 Coupling of bounded and unbounded domains

The force-displacement relationships (Eqs. (19) and (21)) of the bounded and unbounded domains can be assembled together to formulate the equation of motion of the whole system

$$\{f(t)\} = [M_G]\{\ddot{z}(t)\} + [C_G]\{\dot{z}(t)\} + [K_G]\{z(t)\}. \tag{22}$$

The vector of unknowns $\{z(t)\}$ contains the displacements $\{u(t)\}$ of the coupled soil-structure system, the internal variables $\{u^{(1)}\}$ to $\{u^{(M_b)}\}$ corresponding to the bounded domain and the internal variables $\{v^{(1)}\}$ to $\{v^{(M_u)}\}$ of the unbounded domain. The vector $\{f(t)\}$ contains all external forces acting on the coupled soil-structure system. The high-order mass, damping and stiffness matrices $[M_G]$, $[C_G]$ and $[K_G]$ are banded, symmetric and sparse. Equation (22) can be solved using standard time-integration methods.

6 Numerical example

The coupled soil-structure interaction problem shown in Figure 2 is analysed. It consists of an elastic block of width $2b$ and height h, with $2b/h = 2/3$, resting on a homogeneous soil halfspace with shear modulus G_1, mass density ρ_1 and Poisson's ratio $\nu_1 = 0.25$. The shear modulus, mass density and Poisson's ratio of the elastic block are: $G_2 = 9G_1$, $\rho_2 = \rho_1$ and $\nu_2 = 0.25$. Plain strain is assumed.

A uniformly distributed strip load $P(t)$ is acting on the top surface of the block. It's time-dependence and the corresponding Fourier transform are shown in Figure 3. Here, the dimensionless frequency is defined as $a_0 = \omega b/c_{s,1}$ with $c_{s,1}^2 = G_1/\rho_1$.

In the scaled boundary finite element model, the elastic block and a semi-circular near-field portion of the soil of radius b are modelled as two subdomains and discretized with eight nine-node high-order elements. The scaling centre of the unbounded domain is located at the point O shown in Figure 2.

The bounded domain is modelled using the high-order time-domain formulation proposed in Section 3.1. Considering the requirement of 6 nodes per wavelength, the discretization represents $\lambda = 4/3b$. This wavelength corresponds to a maximum dimensionless frequency $a_0 = 14.1$. In the radial direction, 3 to 4 continued- fraction terms per wavelength are required [15]. The order of continued-fraction expansion is thus chosen as $M_b = 3$. The high-order transmitting boundary

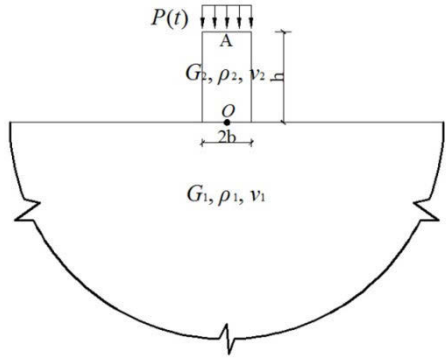

Figure 2: Elastic block resting on homogeneous halfspace

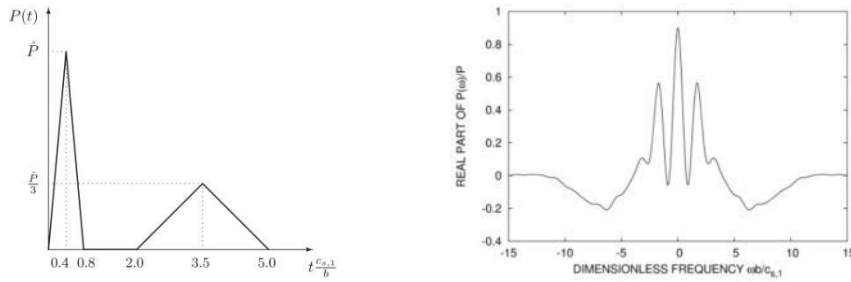

(a) (b)

Figure 3: Uniformly distributed load: (a) time domain, (b) frequency domain

summarized in Section 4 is used to model the far field with $M_u = 9$ and $M_u = 15$. The dimensionless vertical displacements at points A and O (see Figure 2) obtained by solving the coupled Equation (22) with Newmark's method are shown in Figure 4. The time step is $\Delta t = 0.02b/c_{s,1}$.

To verify the proposed method, an extended mesh with a rectangular area of $21b \times 20b$ to the right of the plane of symmetry is analysed using the finite element method (ABAQUS/Standard [18]). Half of the symmetric system is discretized with 6768 eight-node elements of size $0.25b \times 0.25b$, yielding 20657 nodes.

For comparison, a viscous-spring boundary [19] combined with a finite element model of size $8b \times 3b$ is also employed. It consists of parallel connected spring-dashpot systems in the normal and tangential directions, with normal and tangential spring and damping coefficients K_{BN}, C_{BN} and K_{BT}, C_{BT}, respectively.

$$K_{BN} = A\frac{G}{r_b}, \quad C_{BN} = A\rho c_p, \quad K_{BT} = A\frac{G}{2r_b}, \quad C_{BT} = A\rho c_s \tag{23}$$

In Equation (23), the symbols A and r_b denote the total area of all elements around a node at the boundary and the distance from the scattering wave source to the artificial boundary point. Here, r_b is taken as $3b$. The finite element region is discretized with 480 eight-node elements of size $0.25b \times 0.25b$, yielding 1553 nodes.

In Figure 4, the vertical displacements computed using the present coupled method and the viscous-spring boundary agree very well with the extended mesh solution for early times up to $\bar{t} = 5$. After that, the results obtained using the viscous-spring boundary differ considerably from the reference results. On the other hand, the vertical displacements determined using the proposed method agree very well with the reference solution up to $\bar{t} = 10$. The extent of the slight deviations occurring after that depends on the order of continued fraction expansion used in the unbounded domain. The displacements calculated using the present technique

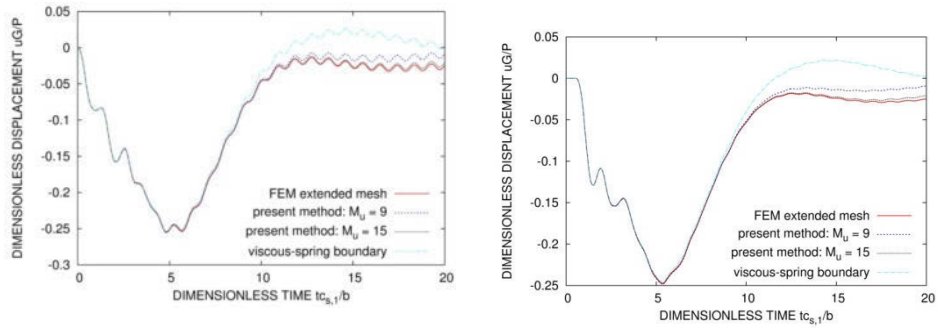

Figure 4: Dimensionless vertical displacements of elastic block on homogeneous halfspace: (a) point A; (b) point O

converge to the extended mesh results with increasing order of continued fraction M_u. In the given example, excellent agreement is obtained using $M_u = 15$.

7 Conclusion

High-order time-domain formulations for modelling wave propagation in bounded and unbounded domains of arbitrary geometry have been developed. A standard equation of motion of a linear system in the time domain is obtained, which can be solved using established time-stepping schemes, such as Newmark's method. Only the boundaries of the bounded and unbounded domains are discretized, leading to reduced numerical effort. The numerical results demonstrate the accuracy of the proposed coupled method. The approach presented in this paper can easily be extended to three-dimensional problems and applied to investigate influence of faults and other geological discontinuities on structural responses.

REFERENCES

[1] Givoli, D.: High-order local non-reflecting boundary conditions: a review; Wave Motion; 39 (2004), Pages 319-326

[2] Kausel, E.: Local transmitting boundaries; Journal of Engineering Mechanics; 114 (1988), Pages 1011-1027

[3] Beskos, D.E.: Boundary element methods in dynamic analysis; Applied Mechanics Reviews; 40 (1987), Pages 1-23

[4] Beskos, D.E.: Boundary element methods in dynamic analysis: Part II (1986-1996); Applied Mechanics Reviews; 50 (1997), Pages 149-197

[5] Bettess, P.: Infinite Elements, Penshaw Press, Sunderland, 1992

[6] Kausel, E.: Thin-layer method: formulation in the time domain; International Journal for Numerical Methods in Engineering; 37 (1994), Pages 927-941

[7] Basu U.; Chopra, A.K.: Perfectly matched layers for transient elastodynamics of unbounded domains; International Journal for Numerical Methods in Engineering; 59 (2004), Pages 1039-1074

[8] Tsynkov, S.V.: Numerical solution of problems on unbounded domains. A review; Applied Numerical Mathematics; 27 (1998), Pages 465-352

[9] Lou, M.L.; Wang, H.F.; Chen X.; Zhai, Y.M.: Soil-structure interaction: Literature review; Soil Dynamics and Earthquake Engineering; 31 (2011), Pages 1724-1732

[10] Komatitsch, D.: Spectral-element simulations of global seismic wave propagation – I. Validation; Geophysical Journal International; 149 (2002), Pages 390-412

[11] Mehdizadeh O.; Paraschivoiu, M.: Investigation of two-dimensional spectral element method for Helmholtz's equation; Journal of Computational Physics; 189 (2003), Pages 111-129

[12] Wolf, J.P.: The scaled boundary finite element method, Wiley & Sons, Chichester, 2003

[13] Song, C.; Wolf, J.P.: The scaled boundary finite element method – alias consistent infinitesimal finite-element cell method – for elastodynamics; Computer Methods in Applied Mechanics and Engineering; 147 (1997), Pages 329-355

[14] Bazyar, M.; Song, C.: A continued-fraction based high-order transmitting boundary for wave propagation in unbounded domains of arbitrary geometry; International Journal for Numerical Methods in Engineering; 74 (2008), Pages 209-237

[15] Song, C.: The scaled boundary finite element method in structural dynamics; International Journal for Numerical Methods in Engineering; 77 (2009), Pages 1139-1171

[16] Birk, C.; Prempramote, S.; Song, C.: An improved continued-fraction-based high-order transmitting boundary for time-domain analyses in unbounded domains; International Journal for Numerical Methods in Engineering; 89 (2012), Pages 269-298

[17] Golub, G.H.; Van Loan, C.F.: Matrix Computations. North Oxford Academic, Oxford, 1983

[18] ABAQUS Inc.: ABAQUS Theory Manual, Version 6.10, Providence, 2010

[19] Deeks, A.J.; Randolph, M.F.: Axisymmetric time-domain transmitting boundaries ; Journal of Engineering Mechanics; 120 (1994), Pages 25-42